JOC The Journal of Organic Chemistry

Article

pubs.acs.org/joc

Colorimetric and Ratiometric Fluorescent Chemosensor Based on Diketopyrrolopyrrole for Selective Detection of Thiols: An Experimental and Theoretical Study

Ling Deng,[†] Wenting Wu,[†] Huimin Guo,[†] Jianzhang Zhao,*[,†] Shaomin Ji,[†] Xin Zhang,[†] Xiaolin Yuan,[‡] and Chunlei Zhang[‡]

[†]State Key Laboratory of Fine Chemicals, School of Chemical Engineering, Dalian University of Technology, E-208 West Campus, 2 Ling-Gong Road, Dalian 116024, P. R. China

[‡]Center Laboratory, Affiliated Zhongshan Hospital of Dalian University, Dalian 116001, P. R. China

Supporting Information

ABSTRACT: A colorimetric and ratiometric fluorescent thiol probe was devised with diketopyrrolopyrrole (DPP) fluorophore. The probe gives absorption and emission at 523 and 666 nm, respectively. In the presence of thiols, such as cysteine, the absorption and emission band shifted to 479 and 540 nm, respectively. Correspondingly, the color of the probe solution changed from purple to yellow, and the fluorescence changed from red to yellow. The emission intensity at 540 nm was enhanced by 140-fold. The Stokes shift of probe **1** (107 nm) is much larger than the unsubstituted DPP fluorophore (56 nm). Mass spectral analysis demonstrated that besides the expected Michael addition of thiols to the C=C bonds, the CN groups of the malonitrile moieties also react with thiols to form 4,5-dihydrothiazole structure. Probe **1** was used for fluorescence imaging of intracellular thiols. In the presence of thiols, both the green and red channel of the microscopy are active. With removal of the intracellular thiols, signal can only be detected through the red channel; thus, ratiometric bioimaging of intracellular thiols was achieved. The ratiometric response of probe **1** was rationalized by DFT calculations. Our complementary experimental and theoretical studies will be useful for design of ratiometric/colorimetric molecular probes.

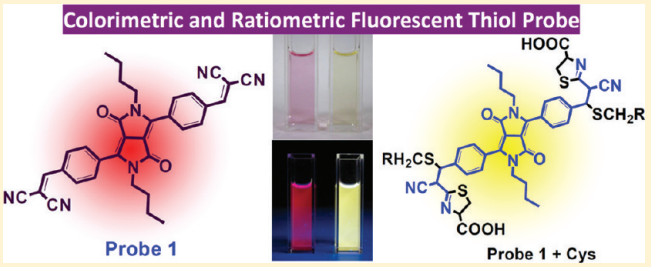

1. INTRODUCTION

Thiols such as cysteine (Cys), homocysteine, glutathione, peptides, and proteins are important for biological science; thus, selective detection of thiols is important.[1] Fluorescence molecular probes have been developed for this purpose because of the high sensitivity and high temporal and spatial resolution of this method.[1−10] Several factors are crucial for successful molecular probe design, such as the appropriate binding site (recognition site), the fluorophore, and the fluorescence transduction mechanism, etc.[11−14] Various fluorophores have been used for fluorescence thiol sensors,[1] such as rhodamine,[15] fluorescein,[16] and BODIPY, etc.[4,5,17,18] The typical fluorescence transduction mechanism is photoinduced electron transfer (PET).[1] However, we noticed some challenges for the development of fluorescent thiols probes.[1] (1) Most of the thiols probes show a fluorescent OFF−ON switching effect. However, ratiometric or colorimetric probes are more desired in order to eliminate the influence of probe concentration on quantification.[19] (2) The fluorophores used for thiol probes are limited to coumarin, fluorescein, rhodamine, or BODIPY.[1] Probes based on other fluorophores were rarely reported. On the other hand, diketopyrrolopyrrole (DPP) is a robust chromophore[20−26] and has been widely used in electromaterials such as organic semiconductors,[27] photovoltaics,[28−32] and two-photon absorption materials,[33,34] but its application in fluorescent molecular probes is very rare.[35,36] (3) Some new sensing mechanisms for thiol probes, such as Michael addition, have been developed, but most of these probes use coumarin as the fluorophore;[37−40] thus, much room is left to fully explore this new sensing mechanism with other fluorophores to improve the photophysical properties of the probes, such as achieving longer emission wavelength, etc. Furthermore, all of the thiol probes based on Michael addition are colorimetric *or* fluorescence OFF−ON probes,[16,19,39,41] and no thiol probes have been developed to *combine* the ratiometric and colorimetric fluorescence transductions.

In order to address the above limitations, herein we use DPP as the fluorophore for thiol probes. In order to design the ratiometric/colorimetric probe, we devised probe **1** (Scheme 1), in which DPP was used as the fluorophore and the malononitrile moiety was introduced. Previously, DPP was only used as the fluorophore for F^- anion and pH sensors.[35,36] To the best of our knowledge, this is the first molecular probe with DPP as the fluorophore to recognize bioactive small organic molecules. The probe is red-emitting. In the presence of thiols,

Received: July 22, 2011
Published: October 18, 2011

dx.doi.org/10.1021/jo201487m | J. Org. Chem. 2011, 76, 9294−9304

Scheme 1. Synthesis of the Thiol Probe 1[a]

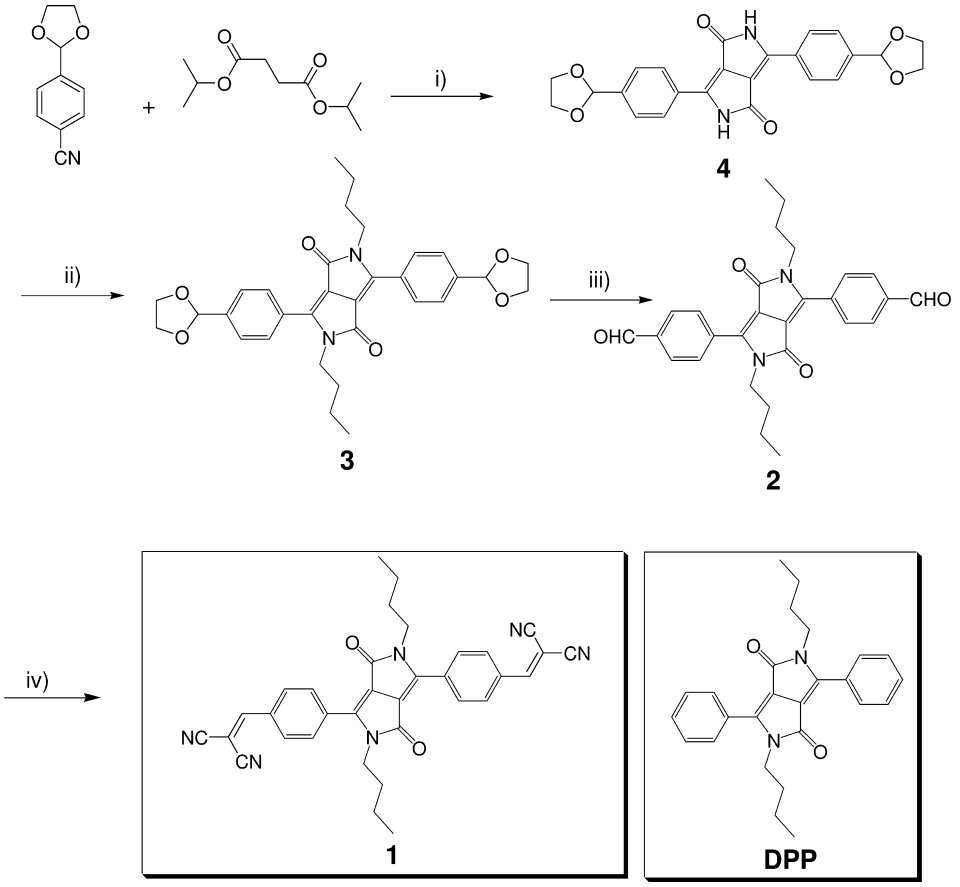

[a]Key: (i) Na, $FeCl_3$, *tert*-amyl alcohol, 100 °C, 24 h, 80%; (ii) potassium *tert*-butoxide, 1-bromobutane, DMF, 60 °C, 12 h, 40%; (iii) THF, 2 M HCl, 60 °C, 2 h 75%; (iv) malononitrile, Al_2O_3, CH_2Cl_2, rt, 30 min, 78%.

such as Cys, yellow emission was observed and the emission intensity was greatly intensified. Furthermore, the solution color of the probe changed from purple to yellow. Thus, the probe simultaneously displays the colorimetric and ratiometric signal transduction. The probe is highly selective toward thiols, and the sensing mechanism, i.e., multiaddition of the thiol molecules to the C═C double bond and the −CN group, was demonstrated by mass spectral analysis. The photophysical properties of the probe, such as UV−vis absorption and fluorescence emission, as well as the ratiometric and the colorimetric signal transduction, were fully rationalized by DFT calculations on the excited states of the fluorophores. We found that the phenyl substituent is in π-conjugation with the DPP fluorophore core; this finding will be useful for future design of molecular probes based on DPPs.

2. RESULTS AND DISCUSSION

2.1. Design and Synthesis of Probe 1 Based on DPP Fluorophore. To the best of our knowledge, DPP has rarely been used as a fluorophore for fluorescent molecular probes.[35,36] Recently, it was shown that the DPP-based chromophore can be used for detection of fluoride anions.[35] Inspired by elegant development of the thiol probes based on Michael addition,[1,16,19] herein we devised probe **1** (Scheme 1), with the intention of obtaining a ratiometric probe because addition of thiols to the C═C double bonds will reduce the electron withdrawal effect of the malonitrile moiety; thus, the UV−vis absorption and emission of chromophore may move to a shorter wavelength. 4-Cyanobenzaldehyde was used as the starting material for the preparation, with the aldehyde group protected by ethylene glycol. Deprotection by HCl leads to the intermediate with biformyl structure. Condensation with malonitrile, under the catalysis of Al_2O_3, gave the probe **1**, which was obtained in satisfying yield (78%) (Scheme 1). It

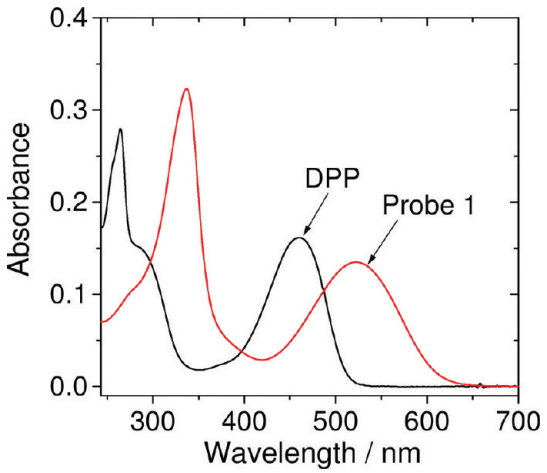

Figure 1. UV−vis absorption spectra of probe **1** and the unsubstituted fluorophore DPP (1.0×10^{-5} mol dm^{-3}). In CH_3CN/H_2O mixed solvent (4/1, v/v), 25 °C.

dx.doi.org/10.1021/jo201487m | *J. Org. Chem.* 2011, 76, 9294−9304

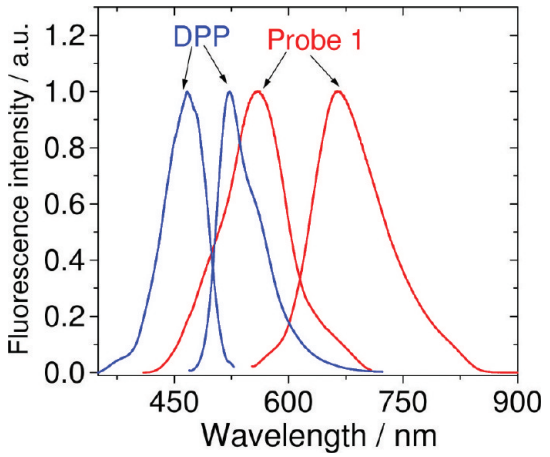

Figure 2. Emission spectra and excitation spectra of probe **1** and DPP. 1.0×10^{-5} mol dm^{-3} of the compounds in CH_3CN/H_2O (v/v= 4/1), 25 °C.

should be pointed out that Al_2O_3 is an efficient catalyst for the condensation reaction.

2.2. Electronic Spectroscopy of the Probe. The UV–vis absorption spectra of the probe and the unsubstituted fluorophore DPP were compared (Figure 1). DPP shows absorption at 461 nm (ε = 16100 M^{-1} cm^{-1}). For probe **1**, however, the absorption band is red-shifted to 523 nm (ε = 13500 M^{-1} cm^{-1}). The red-shift of the absorption band is due to the extended π-conjugation framework of probe **1** vs DPP. The absorption band in the visible region is due to the $\pi-\pi^*$ transition localized on DPP fluorophore. This assignment is supported by the theoretical calculation based on the density functional theory (DFT, see the later section).

The emission and excitation of the compounds were studied (Figure 2). DPP shows an excitation peak at 467 nm and an emission band at 523 nm, respectively. Interestingly, probe **1** shows much red-shifted excitation and emission bands at 559 and 666 nm, respectively. The emission quantum yield of probe **1** (Φ_F = 1.5%, in CH_3CN/H_2O (4:1, v/v)) is much smaller than that of DPP (Φ_F = 75% in CH_3CN/H_2O (4:1, v/v)), but the emission of probe **1** is much stronger in ether (Φ_F = 65%).

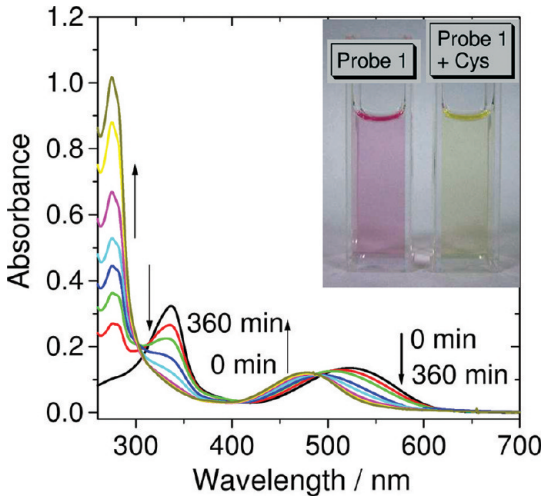

Figure 4. UV–vis absorption of probe **1** before and after addition of Cys. In mixed solvent of CH_3CN/H_2O (4:1, v/v). c (probe **1**) = 1.0×10^{-5} mol dm^{-3}, c (Cys) = 2.0×10^{-3} mol dm^{-3}, 37 °C.

The Stokes shift of probe **1** is 107 nm, much larger than the Stokes shift of DPP (56 nm).

It is known that the emission wavelength of a D–π–A chromophore is sensitive to the polarity of the solvent; i.e., the emission wavelength will show a red-shift in more polar solvents.[6] Such a polarity-dependent emission wavelength is detrimental to the application of ratiometric fluorescence probes in vivo, for which the polarity of the microenvironment is uncontrollable. Thus, the absorption and the emission of probe **1** in solvents with different polarity were studied (Figure 3). The UV–vis absorption spectra show minor variations in different solvents (Figure 3a). For the fluorescence spectra, generally the emission intensity decreased in polar solvents;[6] however, the emission band did not show any shift. The UV–vis absorption and the fluorescence of the fluorophore DPP were also studied, and similar results were observed (Figure S10, Supporting Information). This solvent polarity-independent emission wavelength will be ideal for construction of ratiometric fluorescent molecular probes.

2.3. Spectroscopic Response of Probe 1 to Thiols. The change of the UV–vis absorption of probe **1** in the

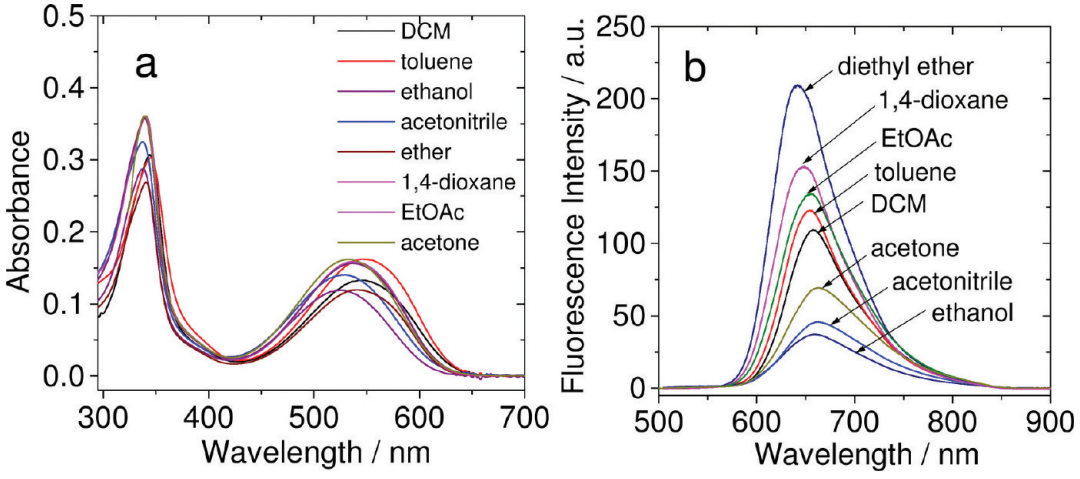

Figure 3. UV–vis absorption and fluorescence spectra of probe **1** in different solvents: (a) UV–vis absorption and (b) fluorescence spectra of **1** (λ_{ex} = 496 nm). c (probe **1**) = 1.0×10^{-5} mol dm^{-3}, 25 °C.

dx.doi.org/10.1021/jo201487m | J. Org. Chem. 2011, 76, 9294–9304

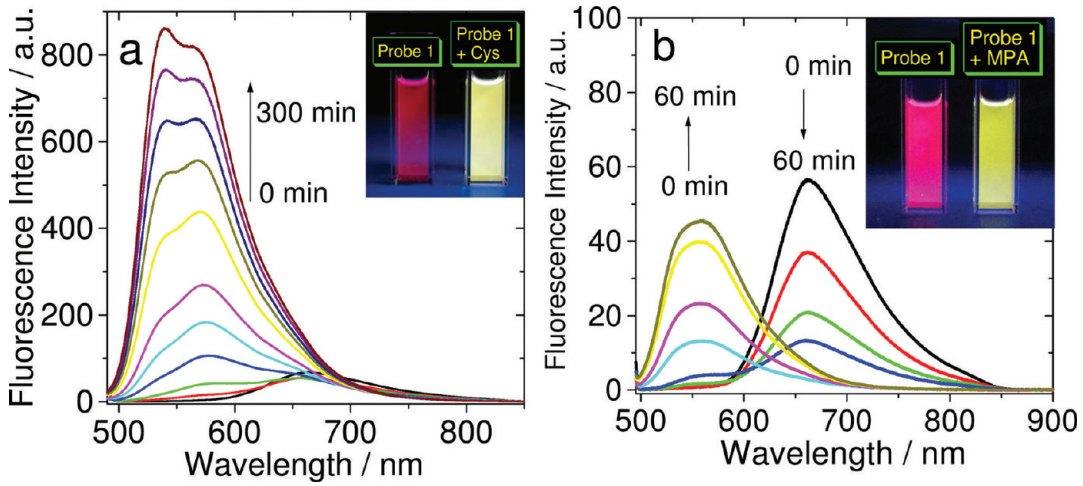

Figure 5. Fluorescence emission spectra of probe **1** in the presence of thiols in different solvents: (a) emission of probe of **1** before and after addition of Cys (λ_{ex} = 490 nm). In mixed solvent of CH_3CN/H_2O (4:1, v/v). (b) emission spectra (λ_{ex} = 490 nm) of probe **1** before and after addition of 3-mercaptopropionic acid (MPA). In CH_3CN. *c* (Probe **1**) = 1.0×10^{-5} mol dm^{-3}, *c* (Cys or 3-mercaptopropionic acid) = 2.0×10^{-3} mol dm^{-3}, 37 °C.

Table 1. Photophysical Parameters of the Probe 1 upon Reaction with Cys

	λ_{abs} (nm)	ε/M^{-1} cm^{-1}	λ_{ex} (nm)	λ_{em} (nm)	Φ_F[a]	τ (ns)
1	523	1.35×10^4	559	666	0.015	6.25
1 + **Cys**	479	1.22×10^4	515	540	0.177	4.37

[a]Quantum yield of fluorescence in CH_3CN/H_2O (4:1, v/v), with quinine sulfate as the standard (Φ = 0.54 in 0.05 M H_2SO_4).

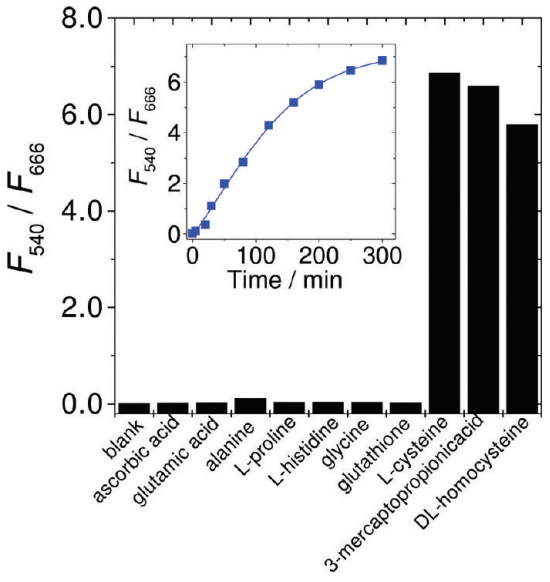

Figure 6. Ratiometric response of probe **1** to different analytes with emission intensiy ratio at 540 and 666 nm. In mixed solvent of CH_3CN/H_2O (4:1, v/v). *c* (probe **1**) = 1.0×10^{-5} mol dm^{-3}, 37 °C. Inset: recognition kinetics of the probe in the presence of Cys.

presence of Cys was studied (Figure 4). In the presence of Cys, the absorption band at 523 nm decreased and a new absorption band at 479 nm developed. Moreover, the absorption band of probe **1** at 337 nm decreased, and a new band at 275 nm developed. The blue-shift of the absorption bands are attributed tentatively to the addition reaction of Cys to the C=C bond of the probe, thus reducing of the π-conjugation framework. Along with the change of absorptions, the color of probe **1** solution was changed from purple to yellow. Compound **1** can be described as a colorimetric probe. A similar response was found for mercaptopropanoic acid and homocysteine (Figure S11, Supporting Information). No response was found for **1** toward nonthiol substrates, such as glutamic acid and ascorbic acid, etc.

The emission changes of the probe in the presence of Cys were studied (Figure 5a). Probe **1** gives weak red emission at 666 nm. In the presence of Cys, a new emission band at 540 nm developed, and the emission intensity at 540 nm was enhanced by 140-fold. Correspondingly, the emission color of the solution changed from deep red to light-yellow. Thus, **1** is a ratiometric probe. To the best of our knowledge, thiol probes that show the *simultaneous* ratiometric and colorimetric spectral changes are rarely reported,[39] and this is the first ratiometric fluorescent thiol probe that is based on fluorophore other than coumarin. Recently, ratiometric thiol probes based on coumarin chromophore were reported, but the emission band was at blue region.[19,42] Although colorimetric thiol probes based on coumarin fluorophore were reported,[37,39] the probe showed a fluorescence OFF−ON effect, not ratiometric fluorescence changes. Probe **1** shows two emission bands in the presence of Cys (Figure 5a), which is proposed on the basis of the reaction product with thiol (for the putative mechanism, see Figure 7).

We noticed that the red emission of probe **1** in protic solvents is weak, but the emission in the presence of Cys is much stronger (Figure 5a). However, we propose that this result does not necessarily mean that the probe can not be used in biological media because the probe may enter the nonprotic hydrophobic micropocket, and then the red-emission and the yellow emission may become more balanced. Balanced emission at two different wavelengths is useful for the ratiometric sensing. Therefore, as a proof of concept, we studied the recognition of thiols with probe **1** in nonprotic solvents (acetonitrile, 3-mercaptopropionic acid was used in stead of Cys, due to the low solubility of Cys in CH_3CN) (Figure 5b). More balanced emission at 558 and 663 nm was observed.

The change of the photophysical properties of probe **1** in the presence of Cys were presented in Table 1. It was found the

dx.doi.org/10.1021/jo201487m | *J. Org. Chem.* 2011, 76, 9294–9304

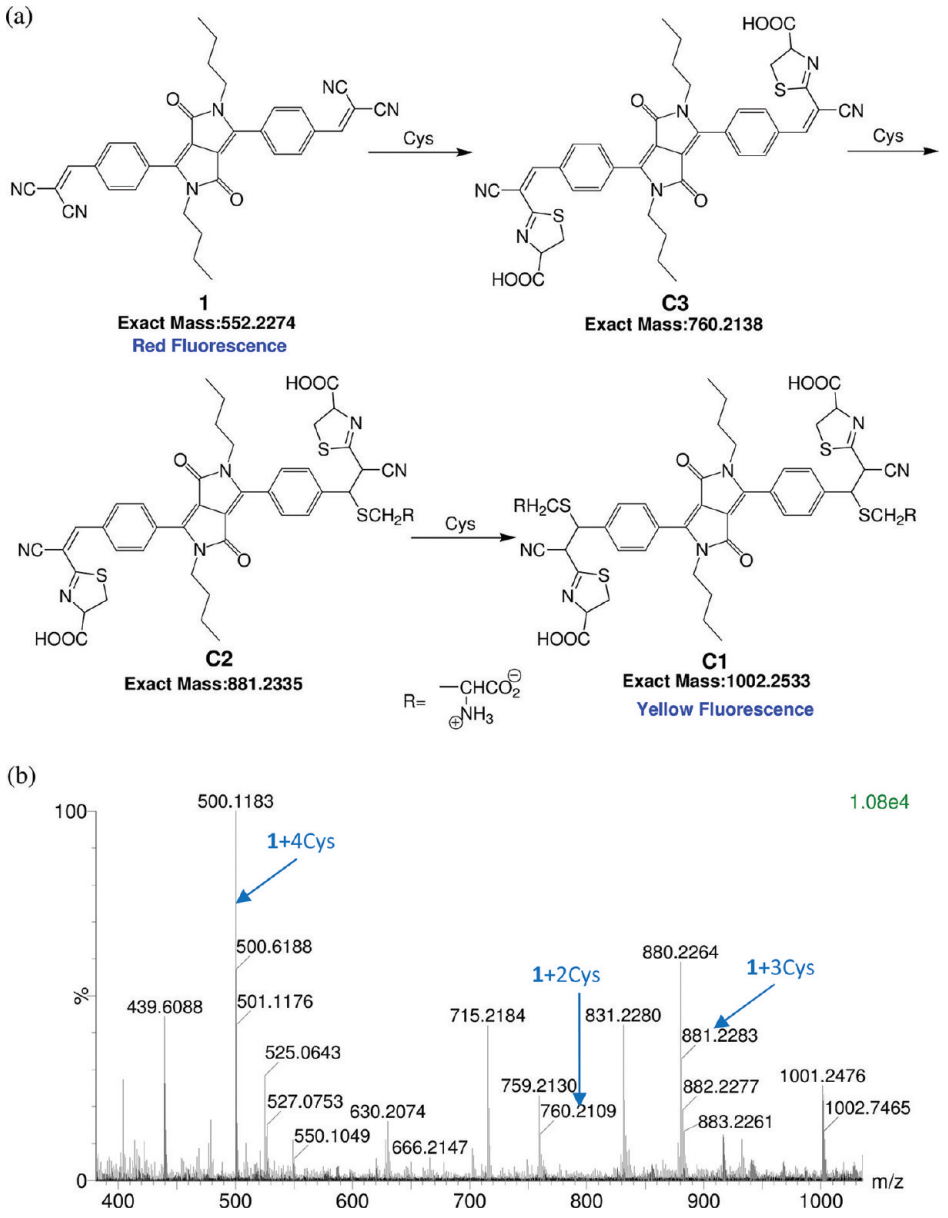

Figure 7. Proposed recognition mechanism of probe **1** toward thiols. (a) Addition of thiols to the probe, demonstrated by Cys. The molecular structures were derived from the mass spectral analysis of the reaction mixtures. (b) TOF-HRMS of **1** upon addition of Cys after 360 min. In CH_3CN/H_2O (4:1, v/v). c(probe 1) = 1.0×10^{-5} mol dm^{-3}, c(Cys) = 2.0×10^{-3} mol dm^{-3}, 37 °C. **C1** (**1** + 4Cys), $[(C_{46}H_{50}N_8O_{10}S_4 - 2H)^{2-}/2]$ calcd 500.1193, found 500.1183; **C2** (**1** + 3Cys), $(C_{43}H_{43}N_7O_8S_3^-)$ calcd 881.2335, found 881.2283; **C3** (**1** + 2Cys), $[(C_{46}H_{36}N_6O_6S_2 - H)^-]$ calcd calcd 760.2138, found 760.2109.

fluorescence quantum yield was increased by 11-fold in the presence of Cys. The blue shift of the emission band is up to 126 nm, which leads to vivid color change of the emission.

The ratiometric responses of the probe toward different analytes are summarized in Figure 6. Probe **1** gives a strong response toward small thiol molecules, such as Cys, mercaptopropionic acid, and homocysteine. No significant responses were found for other analytes. For example, the fluorescence enhancement of probe **1** in the presence of cysteine is ca. 140-fold. The ratiometric response (I_{540nm}/I_{666nm} values, where I_{540nm} and I_{666nm} are the emission intension at 540 and 666 nm in the presence of thiols) is up to 6.8 for Cys. For other biologically related molecules, such as alanine, etc., the response is much smaller (Figure 6). Remarkable responses were observed in the presence of thiols such as 3-mercaptopropionic acid or homocysteine. The detection limit of probe **1** for Cys is determined as 6.02×10^{-7} mol dm^{-3}.

2.4. Sensing Mechanism of Probe 1 Toward Thiols. Initially, we anticipated the normal Michael addition reaction of thiols with probe **1**, i.e., addition of the thiols to the C=C double bonds.[37−39] However, mass spectral analysis of the reaction mixture of the probes with Cys reveals a rather complicated mixture (Figure 7). On the basis of the mass spectra, we propose that up to four Cys molecules can be added to the probe molecule; thus, we propose that the CN group also reacts with Cys. A similar reaction was observed for a polythiophene thiol probe.[43]

2.5. Rationalization of the Colorimetric and Ratiometric Fluorescence Response of Probe 1 toward Thiols. Recently, theoretical calculations have been used for

dx.doi.org/10.1021/jo201487m | J. Org. Chem. 2011, 76, 9294–9304

Table 2. Selected Parameters for the Vertical Excitation (UV−vis Absorptions) and the Fluorescence Emission of Probe 1[a]

		TDDFT//B3LYP/6-31G(d)			
	electronic transitions[b]	excitation energy (eV)	f[c]	composition[d]	CI[e]
absorption	$S_0 \rightarrow S_1$	1.88 (660 nm)	0.8781	H → L	0.7082
	$S_0 \rightarrow S_7$	3.39 (366 nm)	0.9568	H-6 → L	0.1193
				H-4 → L	0.3613
				H-2 → L	0.4753
				H-1 → L+1	0.1157
emission[f]	$S_1 \rightarrow S_0$	1.45 (852 nm)	1.1787	L → H	0.7101

[a]Electronic excitation energies (eV) and oscillator strengths (f), configurations of the low-lying excited states of the probe **1**. Based on the optimized geometries of the ground state and singlet excited state (S_1). Acetonitrile was used as solvent in all of the calculations. Calculated by TDDFT at the B3LYP/6-31G(d) level. [b]Only selected excited states were considered. The numbers in parentheses are the excitation energy in wavelength. [c]Oscillator strength. [d]H stands for HOMO and L stands for LUMO. Only the main configurations are presented. [e]Coefficient of the wave function for each excitations. The CI coefficients are in absolute values. [f]Note the calculation of the emission by TDDFT methods gives the information for the $S_0 \rightarrow S_1$ transition.

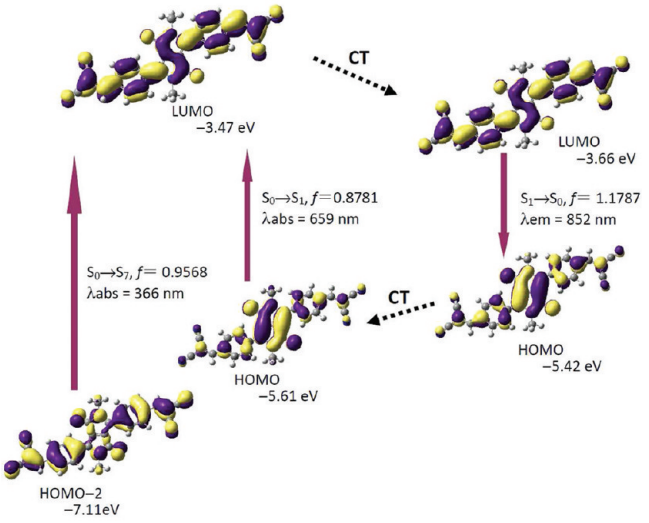

Figure 8. Frontier molecular orbitals (MOs) involved in the vertical excitation (i.e., UV−vis absorption, the left two columns) and the emission (right column) of probe **1**. Acetonitrile was used as solvent for the calculations. The vertical excitation are based on the optimized ground-state geometry (S_0 state, Franck−Condon principle) and the emission-related calculations were based on the optimized excited state (S_1 state, Kasha's rule) at the B3LYP/6-31G(d)//level using Gaussian 09W. Note the energy levels of the HOMO and LUMO at the S_1 state are different from that at the S_0 state. IC stands for internal conversion, and CT stands for conformation transformation. Excitation and radiative processes are marked as solid lines, and the nonradiative processes are marked by dotted lines. Only selected MOs of the transitions are presented; for details, see Table 2.

the study of molecular probes.[4−7,44−48] Previously, we used density functional theory (DFT) and time-dependent DFT (TDDFT) calculations for study of the fluorescence transduction of molecular probes.[4−7,46−48] In principle, the new concept we developed is to use excited state, rather than the molecular orbitals, to study the absorption/emission properties of the molecular probes. Herein we used DFT and TDDFT methods for study of the spectral transduction of probe **1** upon recognition of thiols, i.e., the colorimetric and the ratiometric fluorescence response of the probes in presence of thiols. We found that the blue-shift of UV−vis absorption and the fluorescence in the presence of thiols can be predicted by the TDDFT calculations, based on the ground-state and the excited-state geometries of the compounds, respectively. Furthermore, we found that the biphenyl moieties in the probe are in π-conjugation with the DPP core.

First, the ground-state geometry of probe **1** was optimized. The phenyl ring is tilted by about 29° toward the DPP core. The malonitrile moiety is coplanar with the phenyl moiety. The UV−vis absorption of probe **1** was calculated with the TDDFT method based on the optimized S_0 state geometry. The calculated absorption of probe **1** is at 659 nm, and HOMO→LUMO is the main component of the $S_0 \rightarrow S_1$ transition (Table 2). HOMO is localized on the DPP core, and the LUMO is more distributed on the malonitrile moiety. Thus, the $S_0 \rightarrow S_1$ transition can be described as an intramolecular charge-transfer (ICT) process. The discrepancy between the calculated absorption wavelength and the experimental results is in line with the known fact that the DFT calculations usually underestimate the excitation energy for the transitions with remarkable ICT character.[49,50]

In order to study the emission of probe **1**, the geometry of the lowest lying singlet excited state (S_1 state, which is responsible for fluorescence, Kasha's rule) was optimized. The HOMO/LUMO at the S_1 geometry were presented (Figure 8; note that the MOs will change at different geometries). We found that there is geometry relaxation at the S_1 state compared to the S_0 state geometry. For example, the dihedral angle between the DPP core and the peripheral phenyl ring is 29° at the S_0 state. At the S_1 state, however, the dihedral angle decreased to 21°. Furthermore, the LUMO energy level at the S_1 state is much lower than that at the S_0 state, and the HOMO energy level at the S_1 state is higher than that at S_0 state geometry. The emission transition is basically a CT process; thus, the discrepancy between the calculated emission wavelength (852 nm) and the experimental observations (666 nm) is within expectations.[49,50]

Similarly, the molecular geometry, the UV−vis absorption and fluorescence emission of the adduct of the probe with Cys were studied (Figure 9 and Table 3). The peripheral phenyl ring of the adduct takes a similar dihedral angle toward the DPP core of 31°. The calculated absorption wavelength of the probe **1**−Cys adduct is at 497 nm, which is very close to the experimentally observed 479 nm (Figure 2). We found that compared to the probe, the $S_0 \rightarrow S_1$ transition of the thiol adduct is more localized on the DPP chromophore core.

The geometry of the S_1 state of the probe **1**−Cys adduct was optimized, and we found a geometry relaxation at the S_1 state; i.e., the dihedral angle between the phenyl ring and the DPP core decreased from 31° (ground state) to 19°. Thus, the

dx.doi.org/10.1021/jo201487m | J. Org. Chem. 2011, 76, 9294−9304

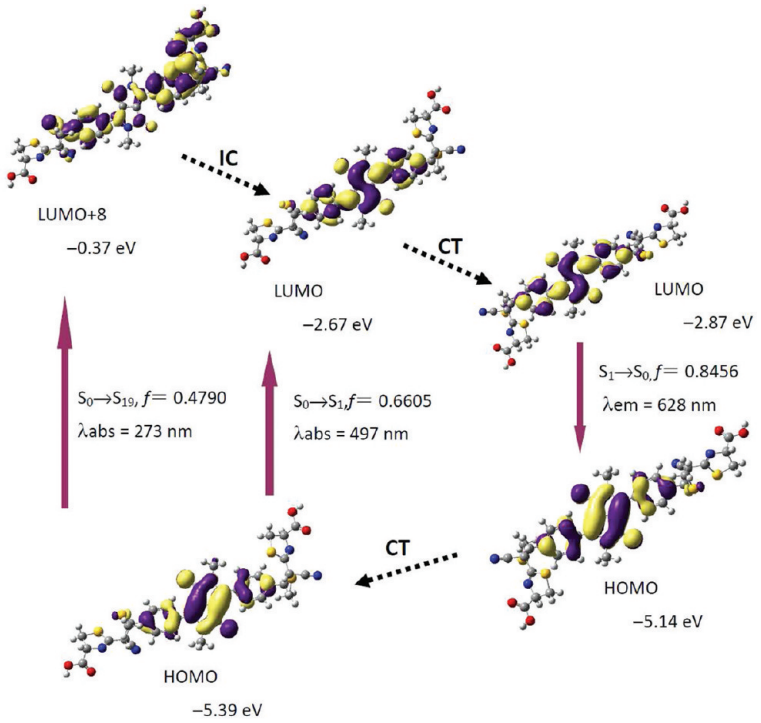

Figure 9. Frontier molecular orbitals (MOs) involved in the vertical excitation (i.e., UV−vis absorption, the left two columns) and emission (right column) of the **1-Cys** adduct (**C-1** in Figure 7, R groups are simplified as H to reduce computation time). Acetonitrile was used as the solvent. The vertical excitation related calculations were based on the optimized ground-state geometry (S_0 state, Franck−Condon principle); the emission related calculations were based on the optimized excited state (S_1 state, Kasha's rule); IC stands for internal conversion and CT stands for conformation transformation. Excitation and radiative processes are marked as solid lines and the nonradiative processes are marked by dotted lines. Only selected MOs are presented; for details see Table 3. All calculations were carried out at the B3LYP/6-31G(d) level using Gaussian 09W.

Table 3. Selected Parameters for the Vertical Excitation (UV−vis Absorptions) and the Fluorescence Emission of the Probe 1−Cys Adduct[a]

		TDDFT//B3LYP/6-31G(d)			
	electronic transitions[b]	excitation energy (eV)	f[c]	composition[d]	CI[e]
absorption	$S_0 \rightarrow S_1$	2.50 (497 nm)	0.6605	H → L	0.7071
	$S_0 \rightarrow S_{19}$	4.55 (273 nm)	0.4790	H-10 → L	0.1218
				H-5 → L+1	0.1604
				H → L+6	0.4519
				H → L+8	0.4565
emission[f]	$S_1 \rightarrow S_0$	1.97 (628 nm)	0.8456	L → H	0.7105

[a]Electronic excitation energies (eV) and oscillator strengths (f), configurations of the low-lying excited states. Calculated by TDDFT//B3LYP/6-31G(d), based on the optimized ground-state geometries and the optimized singlet excited state (S_1). Acetonitrile was employed as solvent in all of the calculations. [b]Only selected excited states were considered. The numbers in parentheses are the excitation energy in wavelength. [c]Oscillator strength. [d]H stands for HOMO and L stands for LUMO. Only the main configurations are presented. [e]Coefficient of the wave function for each excitations. The CI coefficients are in absolute values. [f]Note that the calculation of the emission by TDDFT methods gives the information of $S_0 \rightarrow S_1$ transition.

molecular backbone is more coplanar at the excited state. The calculated emission wavelength is 628 nm. Despite the discrepancy between the theoretically predicted value and the experimental result, the trend is clear; that is, with addition of Cys to the probe, the UV−vis absorption and emission were predicted to move to the higher energy region of the spectrum, in line with the experimental results. Furthermore, the frontier molecular orbitals indicate that the phenyl groups are in π-conjugation with the DPP chromophore. These results may be helpful for design ratiometric fluorescent molecular probes and probes or fluorescent dyes based on DPP core.

In order to validate the DFT calculations on the UV−vis absorption and the fluorescence of the probe **1**−Cys adduct, we also studied the absorption and the fluorescence emission properties of the unsubstituted fluorophore DPP (Figure 10 and Table 4). The theoretically predicted absorption band at 477 nm is in good agreement with the experimental observation at 461 nm. The calculated emission band at 600 nm is red-shifted by ca. 80 nm compared to the experimental results.

Despite of the discrepancy between the calculation and the experimental results, the DFT/TDDFT calculations clearly predicted the blue shift of the absorption and fluorescence of probe **1** upon interaction with thiols, i.e., the colorimetric and ratiometric fluorescence changes. Previously, the fluorescence OFF−ON switching effect was predicted by DFT/TDDFT calculations.[4−7,44,51] To the best of our knowledge, however,

dx.doi.org/10.1021/jo201487m | J. Org. Chem. 2011, 76, 9294−9304

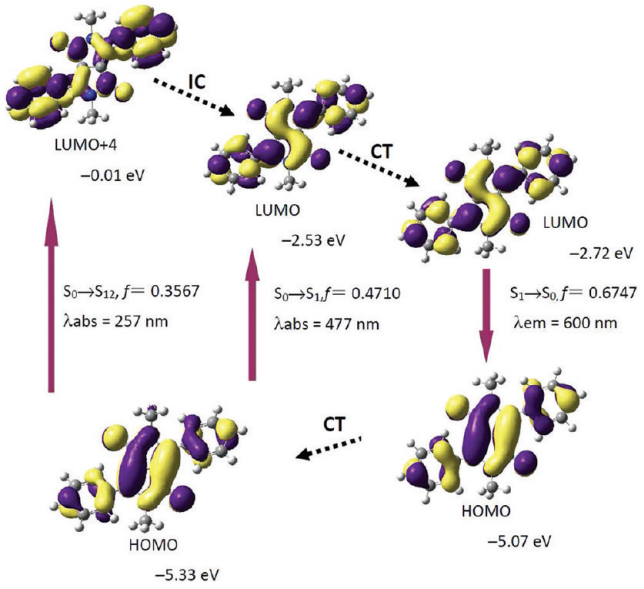

Figure 10. Frontier molecular orbitals (MOs) involved in the vertical excitation (i.e., UV−vis absorption, the left two columns) and emission of diphenyl diketopyrrolopyrrole (DPP) (right column). Acetonitrile was used as the solvent for the calculations. The vertical excitation related calculations were based on the optimized ground-state geometry (S_0 state, Franck-Condon principle), and the emission related calculations were based on the optimized excited state (S_1 state, Kasha's rule). Note that the energy levels of the HOMO and LUMO at S_1 state are different from that at the S_0 state. IC stands for internal conversion, and CT stands for conformation transformation. Excitation and radiative processes are marked as solid lines, and the nonradiative processes are marked by dotted lines. Only selected MOs are presented; for details, see Table 4. Calculations were carried out at the B3LYP/6-31G(d)/ level using Gaussian 09W.

this is the first time that the colorimetric and the ratiometric fluorescence transduction of the molecular probes were studied by the DFT/TDDFT calculations.

The probe **1** was used for fluorescent bioimaging of intracellular thiols (Figure 11). We found that with incubation of MDA-231 cells with probe **1**, both the green channel (Figure 11e) and the red channel (Figure 11f) of the microscope are active, and a yellow image was observed (Figure 11h). With removal of the intracellular thiols by *N*-methylmaleimide, only the red channel is active (Figure 11j) and red emission was detected (Figure 11i). It should be pointed out that ratiometric fluorescent thiol probes are rarely reported.[19,42] The known ratiometric thiol probes gives emission change at shorter wavelength range than probe **1**. For example, emission changed from green to blue color in the presence of thiols.[19,42]

2.6. Conclusions. A colorimetric and ratiometric fluorescent thiol probe was designed with diketopyrrolopyrrole (DPP) as the fluorophore, which shows absorption at 523 nm and a deep red emission at 666 nm. The Stokes shift of the probe (107 nm) is larger than that of the diphenyl DPP fluorophore core (56 nm). In the presence of thiols, the absorption and the emission peaks show 44 and 126 nm blue-shift, respectively. The emission intensity at 540 nm was enhanced by 140-fold in the presence of Cys. Correspondingly, the color of the probe solution changed from purple to yellow, and the fluorescence changed from deep red to yellow upon interaction with thiols. Mass spectra analysis demonstrated that the recognition is based on the Michael addition of thiols to the C=C bond, as well as the −CN groups. To the best of our knowledge, this is the first DPP-based molecular probe to recognize small bioactive organic molecules, and this is also the first thiol probe based on the malonitrile/Michael addition mechanism that show the simultaneous colorimetric and the ratiometric fluorescence changes. The colorimetric and the ratiometric fluorescence changes of the probe **1** upon reaction with thiols were fully rationalized by DFT/TDDFT calculations, based on optimized ground-state (S_0) and excited-state (S_1) geometries (calculation of the absorption and emission wavelengths). Furthermore, we found the emission wavelength of DPP fluorophore is independent of the solvent polarity, which is ideal for fluorophore to construct ratiometric fluorescent molecular probes. The probe was used for fluorescence imaging of intracellular thiols. Both green and red channels can be used for detection of intracellular cells. Without intracellular thiols, only red channel is active. Our complementary experimental and theoretical study will be useful for design of ratiometric and colorimetric molecular probes.

Table 4. Selected Parameters for the Vertical Excitation (UV−vis Absorptions) and the Fluorescence Emission of Diphenyl Diketopyrrolopyrrole (DPP). [a]

		TDDFT//B3LYP/6-31G(d)			
	electronic transitions[b]	excitation energy (eV)	*f*[c]	composition[d]	CI[e]
absorption	$S_0 \rightarrow S_1$	2.60 (477 nm)	0.4710	H →L	0.7079
	$S_0 \rightarrow S_8$	4.11 (302 nm)	0.3862	H-6 → L	0.5602
				H-4 → L	0.2922
				H-2 → L	0.2640
				H → L+4	0.1586
	$S_0 \rightarrow S_{12}$	4.82 (257 nm)	0.3567	H-6 → L	0.1053
				H-1 → L+1	0.2178
				H → L+4	0.6747
emission[f]	$S_1 \rightarrow S_0$	2.07 (600 nm)		L → H	0.7109

[a]Electronic excitation energies (eV) and oscillator strengths (*f*), configurations of the low-lying excited states of DPP, based on the optimized ground-state and the singlet excited-state geometries. Acetonitrile was employed as solvent in all the calculations). Calculated at TDDFT//B3LYP/6-31G(d) level with Gaussian 09W. [b]Only selected excited states were considered. The numbers in parentheses are the excitation energy in wavelength. [c]Oscillator strength. [d]H stands for HOMO, and L stands for LUMO. Only the main configurations are presented. [e]Coefficient of the wave function for each excitations. The CI coefficients are in absolute values. [f]Note the calculation of the emission by TDDFT methods gives the information of $S_0 \rightarrow S_1$ transition.

dx.doi.org/10.1021/jo201487m | *J. Org. Chem.* 2011, 76, 9294–9304

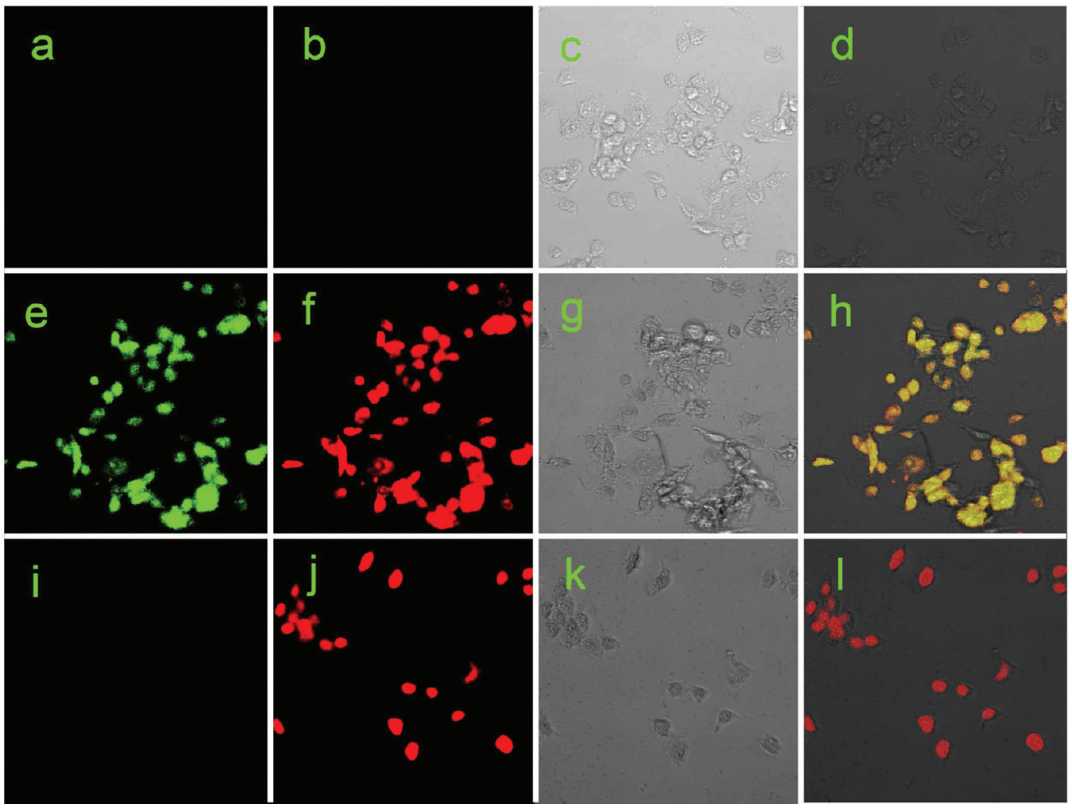

Figure 11. DIC and fluorescence images of living MDA-231 cells. Top panel (a–d): images of the cells without the probe **1**. (a) Fluorescence image of MDA-231 cells from the green channel; (b) fluorescence image of MDA-231 cells from the red channel; (c) DIC image of MDA-231 cells; (d) overlay of images a, b and c. Middle panel (e–h): fluorescence imaging of the intracellular thiols with probe **1**, MDA-231 cells incubated with 10 μM probe **1** for 60 min at 37 °C. (e) Fluorescence image from the green channel after incubation; (f) fluorescence image from the red channel after incubation; (g) DIC image of cells after incubation; (h) overlay of images e–g. Bottom panel (i–l): fluorescence images of the MDA-231 cells pretreated with 1 mM *N*-methylmaleimide for 60 min at 37 °C and then incubated with 10 μM probe **1** for 60 min at 37 °C. (i) Fluorescence image from the green channel; (j) fluorescence image of from the red channel; (k) DIC image and (l) overlay of images i–k.

3. EXPERIMENTAL SECTION

3.1. General Methods. NMR spectra were recorded on a Bruker 400 MHz spectrometer ($CDCl_3$ as solvents, TMS as standard, δ = 0.00 ppm). High-resolution mass spectra (HRMS) were determined on a LC/Q-TOF MS system. Melting points were measured on an X-4 microscopic melting point meter. Fluorescence spectra were measured on a RF5301 PC spectrofluorometer. Fluorescence lifetimes were measured with a OB920 phosphorescence/fluorescence lifetime spectrometer. Absorption spectra were recorded on a UV2550 UV/vis spectrophotometer and an Agilent 8453 UV/vis near-IR spectrophotometer.

3.2. 3,6-Bis[4-1,3-dioxolan-2-ylphenyl]pyrrolo[3,4-*c*]pyrrole-1,4-dione (4).[52] Under argon atmosphere, sodium (1.10 g, 48.0 mmol), $FeCl_3$ (0.05 g), and dry *tert*-amyl alcohol (24 mL) were mixed. The mixture was heated to 100 °C until the sodium disappeared completely. Then 4-(1,3-dioxolan-2-yl)benzonitrile (4.2 g, 24 mmol) was added. A solution of diisopropyl succinate (1.94 g, 9.6 mmol) in dry *tert*-amyl alcohol (10 mL) was added dropwise during 1 h at 100 °C. After the solution was allowed to stand for 24 h at 100 °C, acetic acid (10 mL) was added. After the mixture was allowed to stand for 1 h, the precipitate was filtered and washed with hot water and hot methanol. The red solid was dried under vacuum: yield 4.15 g, 80%; mp 161.5–162.7 °C. EI-HRMS ($C_{24}H_{20}N_2O_6^+$) calcd 432.1321, found 432.1324. No ^{1}H NMR spectrum was measured due to the poor solubility of the compound in common organic solvents.

3.2. 2,5-Dibutyl-3,6-bis[4-1,3-dioxolan-2-ylphenyl]pyrrolo-[3,4-*c*]pyrrole-1,4-dione (3).[52] A mixture of **4** (2.8 g, 6.5 mmol), potassium *tert*-butoxide (1.6 g, 13.9 mmol), and dry DMF (80 mL) was heated to 60 °C, 1-bromobutane (6.5 g, 48 mmol) in DMF (20 mL) was added slowly, and the mixture was stirred at 60 °C for 12 h. After the mixture was cooled to room temperature, dichloromethane (DCM) was added, and then the mixture was washed with water. The organic layer was dried over anhydrous Na_2SO_4, and the solvent was removed under reduced pressure. The product was purified by column chromatography (silica gel; DCM/ethylacetate, 10/1, v/v) to give **3** as an orange solid (1.4 g, 40%): mp 217.7–219.1 °C; ^{1}H NMR (400 MHz, $CDCl_3$) δ 7.82 (d, 4H, J = 8.0 Hz), 7.64 (d, 4H, J = 8.0 Hz), 5.89 (s, 2H), 4.06–4.17 (m, 8H), 3.74 (t, 4H, J = 7.6 Hz), 1.52–1.60 (m, 4H), 1.20–1.30 (m, 4H), 0.84 (t, 6H, J = 7.2 Hz); EI-HRMS ($C_{32}H_{36}N_2O_6^+$) calcd 544.2573, found 544.2571.

3.3. Synthesis of 2,5-Dibutyl-3,6-bis(4-formylphenyl)-pyrrolo[3,4-*c*]pyrrole-1,4-dione (2).[52] A mixture of **3** (1.2 g, 2.2 mmol), THF (20 mL), and HCl (2 M, 10 mL) was stirred for 2 h at 60 °C. After being cooled to room temperature, DCM (60 mL) was added, and the mixture was washed with water and dried over Na_2SO_4. After filtration, the solvent was removed under reduced pressure, and the crude product was purified by column chromatography (silica gel; DCM/ethyl acetate, 10/1, v/v) to give compound **2** (0.75 g, 75%): mp 184.4–186.1 °C; ^{1}H NMR (400 MHz, $CDCl_3$) δ 10.10 (s, 2H), 8.03 (d, 4H, J = 8.0 Hz), 7.97 (d, 4H, J = 8.0 Hz), 3.78 (t, 4H, J = 7.6 Hz), 1.51–1.59 (m, 4H), 1.21–1.31 (m, 4H), 0.84 (t, 6H, J = 7.2 Hz); EI-HRMS ($C_{28}H_{28}N_2O_4^+$) calcd 456.2049, found 456.2052.

3.4. Synthesis of 2,5-Dibutyl-3,6-bis(4-malonitrilephenyl)-pyrrolo[3,4-*c*]pyrrole-1,4-dione (Probe 1). Compound **2** (75 mg, 0.16 mmol), malonitrile (32.5 mg, 0.49 mmol), aluminum oxide (Catalyst. 80 mg), and dry DCM (10 mL) were mixed. The mixture was stirred at room temperature for 30 min. After filtration, the solvent was evaporated, and the crude product was purified by column chromatography (silica gel; DCM/ethylacetate, 15/1, v/v) to give probe **1** as a purple solid (68.9 mg, 78%): mp 279.5–281.1 °C; ^{1}H NMR (400 M Hz, $CDCl_3$) δ 8.07 (d, 4H, J = 8.4 Hz), 8.00 (d, 4H, J =

dx.doi.org/10.1021/jo201487m | *J. Org. Chem.* 2011, 76, 9294–9304

8.4 Hz), 7.81 (s, 2H), 3.79 (t, 4H, J = 7.2 Hz), 1.58−1.60 (m, 4H), 1.26−1.31 (m, 4H), 0.87 (t, 6H, J = 7.2 Hz); ^{13}C NMR (100 MHz, $CDCl_3$) δ 162.4, 158.1, 147.3, 133.3, 133.1, 131.3, 129.8, 113.5, 112.5, 111.9, 84.8, 42.3, 31.8, 20.2, 13.8; EI-HRMS ($C_{34}H_{28}N_6O_2^+$) calcd 552.2274, found 552.2267. Anal. Calcd for $C_{34}H_{28}N_6O_2$ (0.25H_2O): C, 73.30; H, 5.15; N, 15.08. Found: C, 73.39; H, 5.003; N, 15.05.

3.5. Theoretical Calculations. All of the calculations were based on density functional theory (DFT) with B3LYP functional and 6-31G(d) basis set. Acetonitrile was used as solvent in all calculations (PCM model). The UV−vis absorption of the compounds (vertical excitation) were calculated with the TDDFT method based on the optimized ground-state geometry (S_0 state, Franck−Condon principle). For the fluorescence emission, the emission wavelength were calculated based on the optimized excited states geometry (S_1 state, Kasha's rule) by the TDDFT method. All of the calculations were performed with Gaussian 09W.[53]

3.6. Fluorescence Microscopy and Cell-Uptake Studies. MDA-231 cells were grown in RPMI-1640 medium in an atmosphere of 5% CO_2, 95% air at 37 °C. Cells were incubated on 96-well plate and allowed to adhere for 24 h. After 24 h, the cells were washed with PBS (phosphate buffered saline) and then incubated at 37 °C in the presence of probe **1** (10 μM, PBS, pH 7.4) for 60 min. For the control experiment, the MDA-231 cells were pretreated with 1 mM *N*-methylmaleimide in PBS solution (pH 7.4) at 37 °C for 60 min to eliminate all of the free thiols within the cells. After the cells were washed with PBS buffer three times, the maleimide-pretreated cells were incubated at 37 °C in the presence of probe **1** (10 μM, PBS, pH 7.4) for 60 min. Luminescence imaging was performed after the cells were washed three times with PBS buffer. The luminescence images were obtained using a Nikon ECLIPSE-Ti confocal laser scanning microscopy with a 20× objective lens. Green and red luminescence was excited at 488 nm argon laser. The differential interference contrast (DIC) and the fluorescence was captured, digitized and processed with the EZ-C1 Image Examiner software. The images for the thiol-dependent activation and corresponding maleimide controls were taken with identical settings. The wavelength range of the filters used for the microcopy are 515−560 nm for the green channel and 605−680 nm for the red channel, respectively.

■ ASSOCIATED CONTENT

Ⓢ Supporting Information

DFT calculation details, ^{1}H and ^{13}C NMR data of the compounds, photophysical data of the probe, and *z*-matrix of the calculated compounds. This material is available free of charge via the Internet at http://pubs.acs.org.

■ AUTHOR INFORMATION

Corresponding Author

*E-mail: zhaojzh@dlut.edu.cn. Group homepage: http://finechem.dlut.edu.cn/photochem.

■ ACKNOWLEDGMENTS

We thank the NSFC (20972024, 21073028, and 21103015), the Royal Society (UK) and NSFC (China−UK Cost-Share Science Networks, 21011130154), the Fundamental Research Funds for the Central Universities (DUT10ZD212 and DUT11LK19), the Ministry of Education (SRFDP-200801410004 and NCET-08-0077), the State Key Laboratory of Fine Chemicals (KF0802), and the Education Department of Liaoning Province (2009T015) for financial support.

■ REFERENCES

(1) Chen, X.; Zhou, Y.; Peng, X.; Yoon, J. *Chem. Soc. Rev.* **2010**, *39*, 2120−2135.
(2) Xiong, L.; Zhao, Q.; Chen, H.; Wu, Y.; Dong, Z.; Zhou, Z.; Li, F. *Inorg. Chem.* **2010**, *49*, 6402−6408.
(3) Tang, B.; Yin, L.; Wang, X.; Chen, Z.; Tong, L.; Xu, K. *Chem. Commun.* **2009**, 5293−5295.
(4) Guo, H.; Jing, Y.; Yuan, X.; Ji, S.; Zhao, J.; Li, X.; Kan, Y. *Org. Biomol. Chem.* **2011**, *9*, 3844−3853.
(5) Shao, J.; Guo, H.; Ji, S.; Zhao, J. *Biosens. Bioelectron.* **2011**, *26*, 3012−3017.
(6) Ji, S.; Yang, J.; Yang, Q.; Liu, S.; Chen, M.; Zhao, J. *J. Org. Chem.* **2009**, *74*, 4855−4865.
(7) Ji, S.; Guo, H.; Yuan, X.; Li, X.; Ding, H.; Gao, P.; Zhao, C.; Wu, W.; Wu, W.; Zhao, J. *Org. Lett.* **2010**, *12*, 2876−2879.
(8) Lin, W.; Long, L.; Yuan, L.; Cao, Z.; Chen, B.; Tan, W. *Org. Lett.* **2008**, *10*, 5577−5580.
(9) Bouffard, J.; Kim, Y.; Swager, T. M.; Weissleder, R.; Hilderbrand, S. A. *Org. Lett.* **2008**, *10*, 37−40.
(10) Zhang, R.; Yu, X.; Ye, Z.; Wang, G.; Zhang, W.; Yuan, J. *Inorg. Chem.* **2010**, *49*, 7898−7903.
(11) Wright, A. T.; Anslyn, E. V. *Chem. Soc. Rev.* **2006**, *35*, 14−28.
(12) James, T. D. *Top. Curr. Chem.* **2007**, *277*, 107−152.
(13) Kim, D.; Chung, Y.; Jun, M.; Ahn, K. H. *J. Org. Chem.* **2009**, *74*, 4849−4854.
(14) Ryu, D.; Park, E.; Kim, D.; Yan, S.; Lee, J. Y.; Chang, B.; Ahn, K. H. *J. Am. Chem. Soc.* **2008**, *130*, 2394−2395.
(15) Li, H.; Fan, J.; Wang, J.; Tian, M.; Du, J.; Sun, S.; Sun, P.; Peng, X. *Chem. Commun.* **2009**, 5904−5906.
(16) Chen, X.; Ko, S.; Kim, M. J.; Shin, I.; Yoon, J. *Chem. Commun.* **2010**, 2751−2753.
(17) Matsumoto, T.; Urano, Y.; Shoda, T.; Kojima, H.; Nagano, T. *Org. Lett.* **2007**, *9*, 3375−3377.
(18) Li, X.; Qian, S.; He, Q.; Yang, B.; Li, J.; Hu, Y. *Org. Biomol. Chem.* **2010**, *8*, 3627−3630.
(19) Kim, G.; Lee, K.; Kwon, H.; Kim, H. *Org. Lett.* **2011**, *13*, 2799−2801.
(20) Bürckstümmer, H.; Weissenstein, A.; Bialas, D.; Würthner, F. *J. Org. Chem.* **2011**, *76*, 2426−2432.
(21) Zhang, G.; Liu, K.; Li, Y.; Yang, M. *Polym. Int.* **2009**, *58*, 665−673.
(22) Luňák, S. Jr.; Vyňuchal, J.; Vala, M.; Havel, L.; Hrdina, R. *Dyes Pigments* **2009**, *82*, 102−108.
(23) Kuwabara, J.; Yamagata, T.; Kanbara, T. *Tetrahedron* **2010**, *66*, 3736−3741.
(24) Celik, S.; Ergun, Y.; Alp, S. *J. Fluoresc.* **2009**, *19*, 829−835.
(25) Vala, M.; Vyňuchal, J.; Toman, P.; Weiter, M.; Luňák, S. Jr. *Dyes Pigments* **2010**, *84*, 176−182.
(26) Stas, S.; Sergeyev, S.; Geerts, Y. *Tetrahedron* **2010**, *66*, 1837−1845.
(27) Suraru, S.; Zschieschang, U.; Klauk, H.; Würthner, F. *Chem. Commun.* **2011**, 1767−1769.
(28) Wienk, M. M.; Turbiez, M.; Gilot, J.; Janssen, R. A. J. *Adv. Mater.* **2008**, *20*, 2556−2560.
(29) Chen, G.; Chiang, C.; Kekuda, D.; Lan, S.; Chu, C.; Wei, K. *J. Polym. Sci., Part A: Polym. Chem.* **2010**, *48*, 1669−1675.
(30) Woo, C. H.; Beaujuge, P. M.; Holcombe, T. W.; Lee, O. P.; Fréchet, J. M. J. *J. Am. Chem. Soc.* **2010**, *132*, 15547−15549.
(31) Falzon, M.; Zoombelt, A. P.; Wienk, M. M.; Janssen, R. A. J. *Phys. Chem. Chem. Phys.* **2011**, *13*, 8931−8939.
(32) Kanimozhi, C.; Balraju, P.; Sharma, G. D.; Patil, S. *J. Phys. Chem. B* **2010**, *114*, 3095−3103.
(33) Guo, E.; Ren, P.; Zhang, Y.; Zhang, H.; Yang, W. *Chem. Commun.* **2009**, 5859−5861.
(34) Jiang, Y.; Wang, Y.; Hua, J.; Qu, S.; Qian, S.; Tian, H. *J. Polym. Sci., Part A: Polym. Chem.* **2009**, *47*, 4400−4408.
(35) Qu, Y.; Hua, J.; Tian, H. *Org. Lett.* **2010**, *12*, 3320−3323.
(36) Yamagata, T.; Kuwabara, J.; Kanbara, T. *Tetrahedron Lett.* **2010**, *51*, 1596−1599.
(37) Kwon, H.; Lee, K.; Kim, H. *Chem. Commun.* **2011**, 1773−1775.
(38) Yi, L.; Li, H.; Sun, L.; Liu, L.; Zhang, C.; Xi, Z. *Angew. Chem. Int. Ed.* **2009**, *48*, 4034−4037.
(39) Jung, H.; Ko, K.; Kim, G.; Lee, A.; Na, Y.; Kang, C.; Lee, J.; Kim, J. *Org. Lett.* **2011**, *13*, 1498−1501.

(40) Lin, W.; Yuan, L.; Cao, Z.; Feng, Y.; Long, L. *Chem.—Eur. J.* **2009**, *15*, 5096−5103.
(41) Huo, F.; Sun, Y.; Su, J.; Chao, J.; Zhi, H.; Yin, C. *Org. Lett.* **2009**, *11*, 4918−4921.
(42) Yuan, L.; Lin, W.; Yang, Y. *Chem. Commun.* **2011**, *47*, 6275−6277.
(43) Yao, Z.; Bai, H.; Li, C.; Shi, G. *Chem. Commun.* **2011**, *47*, 7431−7433.
(44) Kowalczyk, T.; Lin, Z.; Voorhis, T. V. *J. Phys. Chem. A* **2010**, *114*, 10427−10434.
(45) Larkin, J. D.; Fossey, J. S.; James, T. D.; Brooks, B. R.; Bock, C. W. *J. Phys. Chem. A* **2010**, *114*, 12531−12539.
(46) Han, F.; Chi, L.; Liang, X.; Ji, S.; Liu, S.; Zhou, F.; Wu, Y.; Han, K.; Zhao, J.; James, T. D. *J. Org. Chem.* **2009**, *74*, 1333−1336.
(47) Zhang, X.; Chi, L.; Ji, S.; Wu, Y.; Song, P.; Han, K.; Guo, H.; James, T. D.; Zhao, J. *J. Am. Chem. Soc.* **2009**, *131*, 17452−17463.
(48) Zhang, X.; Wu, Y.; Ji, S.; Guo, H.; Song, P.; Han, K.; Wu, W.; Wu, W.; James, T. D.; Zhao, J. *J. Org. Chem.* **2010**, *75*, 2578−2588.
(49) Wu, C.; Tretiak, S.; Chernyak, V. Y. *Chem. Phys. Lett.* **2007**, *433*, 305−311.
(50) Dreuw, A.; Head-Gordon, M. *J. Am. Chem. Soc.* **2004**, *126*, 4007−4016.
(51) Gabe, Y.; Urano, Y.; Kikuchi, K.; Kojima, H.; Nagano, T. *J. Am. Chem. Soc.* **2004**, *126*, 3357−3367.
(52) Jin, Y.; Xu, Y.; Liu, Y.; Wang, L.; Jiang, H.; Li, X.; Cao, D. *Dyes Pigm.* **2011**, *90*, 311−318.
(53) Frisch, M. J.; Trucks, G. W.; Schlegel, H. B.;et al. *Gaussian 09W Revision A.1*, Gaussian Inc., Wallingford, CT, 2009.